Absorption spectra of dipolar Frenkel excitons in two-dimensional lattices with configurational disorder: Long-range interaction and motional narrowing effects

F. Domnguez-Adame, V. A. Malyshev, and A. Rodrguez

Citation: The Journal of Chemical Physics **112**, 3023 (2000); doi: 10.1063/1.480876
View online: http://dx.doi.org/10.1063/1.480876
View Table of Contents: http://scitation.aip.org/content/aip/journal/jcp/112/6?ver=pdfcov
Published by the AIP Publishing

Absorption spectra of dipolar Frenkel excitons in two-dimensional lattices with configurational disorder: Long-range interaction and motional narrowing effects

F. Domínguez-Adame[a] and V. A. Malyshev[b]
GISC, Departamento de Física de Materiales, Universidad Complutense, E-28040 Madrid, Spain

A. Rodríguez
GISC, Departamento de Matemática Aplicada y Estadística, Universidad Politécnica, E-28040 Madrid, Spain

(Received 18 May 1999; accepted 9 November 1999)

We present results of numerical simulations of optical absorption line shape of Frenkel excitons in two-dimensional disordered lattices. Disorder is generated by Gaussian randomness in the molecular positions. The intersite interaction is considered to be of dipole origin, including coupling to far neighbors. Results of simulations are compared with those obtained in the frame of the nearest-neighbor approximation, showing remarkable differences in the absorption line shape. The motional narrowing effect is found to be essentially different from that previously reported for the case of diagonal disorder as well as for that produced by randomness in nearest-neighbor hopping integrals. © *2000 American Institute of Physics.* [S0021-9606(00)53105-5]

I. INTRODUCTION

A number of physical phenomena in insulating and molecular crystals involve the concept of Frenkel excitons for their explanation.[1] In past years, the framework of one-dimensional (1D) exciton states was successfully applied to treating optical properties of linear molecular *J*-aggregates of cyanine dyes (see Refs. 2 and 3 and references therein for review). Optical dynamics of excitations in quasi-two-dimensional molecular systems such as Langmuir–Blodgett films comprised of cyanine dyes was also interpreted in terms of two-dimensional (2D) Frenkel exciton states.[4–7] Very recently, a 2D model was used for studying the time-dependent energy transfer in a Sheibe aggregate.[8] Solitary exciton waves have been predicted in 1D[9–12] and 2D Frenkel lattices.[13]

The nearest-neighbor (NN) approximation is often adopted in analytical and numerical studies of the optical dynamics of Frenkel excitons, independently of the system dimensionality. It was found that, even in the 1D geometry, coupling to far neighbors has nonperturbative effects on the exciton eigenenergies and eigenstates close to the bottom as well as the top of the exciton band;[5,14–17] these peculiarities are also reflected in the optical response and transport properties of 1D Frenkel excitons. It is then rather reasonable to expect similar or even larger effects for 2D Frenkel systems.

In this paper, we focus on 2D Frenkel excitons in random molecular systems, assuming that disorder arises from randomness in positions of molecules around regular lattice points and neglecting the static inhomogeneous offset energy of molecules imposed by the surrounding host medium (diagonal disorder). We do not restrict ourselves to NN interactions but keep the long-range dipole–dipole terms as well, showing that these terms and configurational disorder strongly affect the exciton absorption line shape.

The remainder of the paper is organized as follows. The model we will be dealing with is described in Sec. II. In Sec. III we briefly overview the basic formalism for calculating the one-exciton absorption line shape. Section IV presents the effects of long-range dipole–dipole coupling on energetic and optical properties of excitons for an ordered 2D lattice, either infinite or finite. Section V deals with an analytical approach as well as the numerical simulations of the exciton absorption lines for configurationally disordered 2D lattices. We summarize our findings in Sec. VI. The Appendix provides the details of the analytical treatment of peculiarities of the motional narrowing effect due to configurational disorder.

II. MODEL HAMILTONIAN

We consider a system of $\mathcal{N}=N\times N$ optically active, two-level molecules, occupying positions $\mathbf{r_n}$ around a regular 2D square lattice with spacing unity. In the absence of diagonal disorder, the effective Frenkel Hamiltonian describing this system can be written as follows:

$$\mathcal{H}=\sum_{\mathbf{mn}} J_{\mathbf{nm}}\, a_{\mathbf{n}}^{\dagger} a_{\mathbf{m}}. \tag{1}$$

Here, $a_{\mathbf{n}}^{\dagger}$ and $a_{\mathbf{n}}$ create and annihilate an electronic excitation of molecule $\mathbf{n}$, respectively. The coupling $J_{\mathbf{nm}}(\mathbf{n}\neq\mathbf{m})$ is the intersite interaction of dipole origin between centers $\mathbf{n}$ and $\mathbf{m}$ $(J_{\mathbf{nn}}\equiv 0)$. Hereafter, we assume that transition dipole moments are perpendicular to the plane of the system and that their magnitudes are the same. Thus, the intersite interaction is found to be of the form $J_{\mathbf{nm}}=J/|\mathbf{r_n}-\mathbf{r_m}|^3$, where $J>0$ is the coupling between NN centers in the regular lattice. For

[a]Electronic mail: adame@valbuena.fis.ucm.es
[b]On leave from All-Russian Research Center ''Vavilov State Optical Institute,'' Saint Petersburg, Russia.

$J>0$, the state coupled to the light is that at the top of the exciton band. Rigorously speaking, the optical dynamics of excitons in such a case can be substantially affected by the coupling to phonons.[18] In this paper, we do not aim to present a complete description of the problem but mainly focus our attention on the effects of coupling to far neighbors on the one-exciton absorption spectrum of 2D Frenkel excitons, just to demonstrate the relevance of the long-range tail of the dipole–dipole interaction.

The source of disorder lies in the interaction terms $J_{\mathbf{nm}}$ caused by randomness in the molecular positions, the distribution of each one being assumed Gaussian

$$P(\boldsymbol{\xi}_{\mathbf{n}})=\frac{1}{2\pi\sigma^2}\exp\left(-\frac{\boldsymbol{\xi}_{\mathbf{n}}^{\,2}}{2\sigma^2}\right), \tag{2}$$

where $\boldsymbol{\xi}_{\mathbf{n}}=\mathbf{r}_{\mathbf{n}}-\mathbf{n}$ and $\mathbf{n}=(n_x,n_y)$ with $1\leqslant n_x,\ n_y\leqslant N$ being integers. For the sake of simplicity, the same standard deviation σ along both directions has been taken, but different values can be considered as well in our model. We do not assume any correlation in the fluctuations of different positions, so that the distribution function of a realization of disorder is represented by the direct product of single Gaussians (2).

III. ONE-EXCITON ABSORPTION SPECTRUM

Having presented our model, we now describe two methods we have used to calculate the absorption spectra. First, the absorption line shape $I(E)$ of a one-exciton transition we will be interested in for this paper can be obtained as follows. Let us consider the total dipole moment operator $\mathcal{D}=\Sigma_{\mathbf{n}}(a_{\mathbf{n}}^{\dagger}+a_{\mathbf{n}})$, where the dipole moment of each center is taken to be unity. Here we are restricting ourselves to the case of systems whose length is much smaller than the optical wavelength. Denote the eigenvectors and eigenvalues of the Hamiltonian $\mathcal{H}$ by $|k\rangle$ and E_k, respectively. Then, the one-exciton absorption spectrum is given by

$$I(E)=\frac{1}{\mathcal{N}}\sum_k |\langle k|\mathcal{D}|\mathrm{vac}\rangle|^2\delta(E-E_k), \tag{3}$$

where the state $|\mathrm{vac}\rangle$ stands for the exciton vacuum. In practice, one considers a broadened δ function, replacing the proper δ function by a Lorentzian distribution of half-width α

$$\delta(E-E_k)\to\frac{\alpha}{\pi}\frac{1}{\alpha^2+(E-E_k)^2}.$$

The dissipation parameter α mimics the always present relaxation.

The use of Eq. (3) for calculations of the one-exciton absorption spectrum implies diagonalization of the Hamiltonian (1). Huber and Ching[19] proposed an alternative (time-domain) method for obtaining this spectrum based on the exciton Green function. It consists of the following. Using the representation

$$\frac{\alpha}{\alpha^2+(E-E_k)^2}=\mathrm{Re}\int_0^\infty dt\, e^{-\alpha t+i(E-E_k)t},$$

Eq. (3) can be rewritten in the form

$$I(E)=\frac{1}{\pi\mathcal{N}}\mathrm{Re}\left[\int_0^\infty dt\, e^{-\alpha t+iEt}\sum_{\mathbf{n}} G_{\mathbf{n}}(t)\right]. \tag{4}$$

Here, we have introduced the Green function $G_{\mathbf{n}}(t)$ according to[19]

$$G_{\mathbf{n}}(t)=\langle\mathrm{vac}|a_{\mathbf{n}}e^{-i\mathcal{H}t}D|\mathrm{vac}\rangle. \tag{5}$$

This function obeys the equation of motion

$$i\frac{d}{dt}G_{\mathbf{n}}(t)=\sum_{\mathbf{m}} J_{\mathbf{nm}}G_{\mathbf{m}}(t). \tag{6}$$

Initial conditions read $G_{\mathbf{n}}(0)=1$ and free-end boundary conditions are used. The microscopic equation of motion is a 2D discrete Schrödinger-like equation on a lattice, and standard numerical techniques may be applied to obtain the solution. Once the equation of motion is solved, the line shape is found from Eq. (4).

For the infinite lattice, both definitions (3) and (4) give a self-averaged quantity. For a finite lattice, one should make the average of Eqs. (3) and (4) over the ensemble of realizations of disorder or, in other words, over the probability distribution given by $\Pi_{\mathbf{n}}P(\boldsymbol{\xi}_{\mathbf{n}})$ with $P(\boldsymbol{\xi}_{\mathbf{n}})$ defined in (2).

IV. ORDERED LATTICE

A. Infinite lattice

In this section, we discuss the case of an infinite lattice where molecules are placed over regular lattice points ($\sigma=0$). This task is instructive in order to compare our model with those based on the NN approximation. The microscopic equation of motion (6) reduces in this case to

$$i\frac{d}{dt}G_{\mathbf{n}}(t)=J\sum_{\mathbf{m}}\frac{1}{|\mathbf{m}-\mathbf{n}|^3}G_{\mathbf{m}}(t), \tag{7}$$

where $\mathbf{m}$ and $\mathbf{n}$ run over the regular lattice sites, excluding singular terms ($\mathbf{m}\neq\mathbf{n}$). It can be solved by means of the Fourier transformation

$$G_{\mathbf{n}}(t)=\sum_{\mathbf{k}\in\mathrm{BZ}} e^{i\mathbf{k}\cdot\mathbf{n}}G_{\mathbf{k}}(t), \tag{8}$$

where BZ refers to the first Brillouin zone: $-\pi<k_x,\ k_y\leqslant\pi$. The calculation is straightforward and gives the following result:

$$G_{\mathbf{n}}(t)=\exp(-iE_0t), \tag{9}$$

where $E_0\equiv E_{\mathbf{k}=\mathbf{0}}$ and

$$E_{\mathbf{k}}=J\sum_{\mathbf{n}\neq\mathbf{0}}\frac{1}{|\mathbf{n}|^3}e^{i\mathbf{k}\cdot\mathbf{n}} \tag{10}$$

is just the exciton energy spectrum. After inserting (9) in (4), the one-exciton absorption spectrum is found to consist of a single line centered at the energy

$$E_0=J\mathcal{F}_3, \tag{11}$$

where for brevity we have introduced the notation

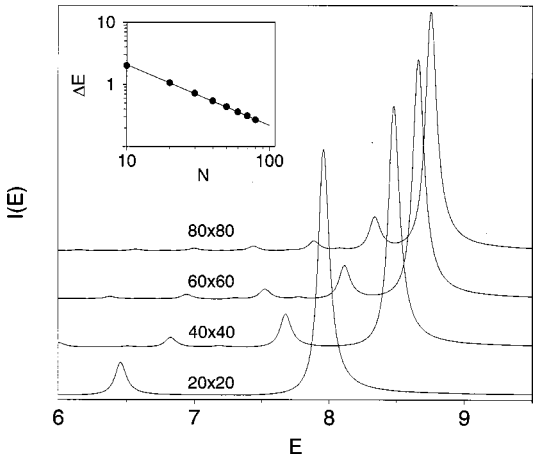

FIG. 1. Absorption spectra in arbitrary units for finite ordered 2D lattices of different sizes when dipole–dipole interaction between all sites is taken into account. Curves are calculated by means of the Green function method with $J=1$ and $\alpha=0.05$ and have equal area. Inset shows the energy shift $\Delta E \equiv E_0 - E$ as a function of the lateral size.

$$\mathcal{F}_l = \sum_{\mathbf{n}} \frac{1}{|\mathbf{n}|^l} = 4\zeta(l/2)\beta(l/2). \tag{12}$$

Here, $\zeta(s)=\Sigma_{n=1}^{\infty} n^{-s}$ is the Riemann's zeta function and $\beta(s)=\Sigma_{n=0}^{\infty}(-1)^n(2n+1)^{-s}$ is the analytical continuation of the Dirichlet series.[13,20] Thus, $\mathcal{F}_3=4\xi(3/2)\times\beta(3/2)=9.03,...$ It is worth mentioning that this energy is rather different from that obtained in the NN approximation. This approximation considers only the four terms with $|\mathbf{n}|=1$ in the sum appearing in (12), the energy of the main line thus being $4J$ instead of $9.03J$. Therefore, we are led to the conclusion that the NN approximation largely underestimates the value of the blueshift.

The exact exciton spectrum (10) near the top of the band also strongly differs from that in the NN approximation given by

$$E_{\mathbf{k}} = 2J[\cos(k_x)+\cos(k_y)] \simeq 4J - J\mathbf{k}^2. \tag{13}$$

As it was found in Ref. 13, for $|\mathbf{k}| \ll 1$ Eq. (10) reduces to

$$E_{\mathbf{k}} \simeq 9.03J - 2\pi J|\mathbf{k}|, \tag{14}$$

i.e., the exact exciton energy $E_{\mathbf{k}}$ scales linearly as $|\mathbf{k}|$, contrary to the parabolic law for the NN model.

B. Finite lattice

Once the infinite ordered lattice has been discussed, we turn our attention to the finite one. We have solved numerically the microscopic equation of motion (6) using the fourth-order Runge–Kutta method. The calculations have been carried out choosing $J=1$ and $\alpha=0.05$. The maximum integration time was 150 in these units and the number of time steps was 12 000. Figure 1 shows the absorption spectra for different system sizes, indicated on each curve. We notice that the main absorption line is blueshifted upon increasing the lattice size. For the largest lattice (80×80), it is centered at $E=8.76$, rather close to the main line in an infinite lattice ($E_0=9.03$). The energy shift between the main line of the infinite lattice and the main line of the $N\times N$ lattice scales as $\sim N^{-1}$ (see inset of Fig. 1) as deduced from (14).

Besides the main line, several almost equidistant and well-defined satellite peaks appear in the low-energy side of the spectra. We relate these peaks to transitions to lower exciton states having oscillator strength smaller than the main transition (to the top band state), similar to what occurs in a finite linear chain (see, for instance, Ref. 14). The relative intensities of peaks are in a good correspondence to the sequence $1/(2n-1)^2$ with $n=1,2,...$, as occurs for a linear chain as well. For $N=80$, the sequence of peaks is fitted surprisingly well by the expression (14) for the infinite lattice by replacing $\mathbf{k}$ in the first Brillouin zone by $\mathbf{k}=[\pi\nu_x/(N+1),\pi\nu_y/(N+1)]$, where ν_x, $\nu_y=1,2,...,N$. In particular, the first three peaks in Fig. 1 have energies 8.76, 8.33, and 7.88 in order of decreasing intensity. The energies, calculated from Eq. (14) by taking (ν_x,ν_y) as the following sets (1,1), (1,3), and (1,5) for $N=80$, appear to be 8.69, 8.27, and 7.80, respectively. These findings are unambiguous evidence that the corresponding 2D exciton states $\Psi_{\nu\mathbf{n}}$ can be approximately expressed as products of the 1D exciton states

$$\varphi_{\nu_i,n_i} = \left(\frac{2}{N+1}\right)^{1/2} \sin\left(\frac{\pi\nu_i n_i}{N+1}\right), \quad i=x,y \tag{15}$$

despite the fact that the 2D exciton energy spectrum (14) is not parabolic and thus the motion of excitons along x and y directions is not independent of each other. It should be noticed that such a correspondence becomes, however, worse as the lattice size decreases. Observing the spectra presented in Fig. 1, one can identify more satellites with very low intensities which are visible nevertheless. Fitting their energies in the same manner as above showed that they can be related approximately to the sets (1,4) and (1,6). Since the oscillator strengths of 1D exciton states with $\nu_y=4,6$ are rigorously equal to zero, we believe that the 2D states now discussed are composed of the 1D state $\nu_x=1$ and of the states $\nu_y=4$ and $\nu_y=6$ mixed perturbatively with the former.

V. DISORDERED LATTICE

Having discussed the regular lattice, we now turn to disordered lattices ($\sigma\neq0$) to analyze the effect of randomness in molecular positions on the width and shift of the absorption line. Our task is to calculate the averaged Green function $\langle G_{\mathbf{n}}\rangle$, where brackets denote the average over realizations of disorder. The coherent potential approximation[21] is widely used for this aim. It has been successfully applied for describing the optical characteristics of Frenkel excitons in the presence of randomness in the transition energies[19,22,23] as well as for theoretical studies of coupled spin systems with randomness in the intersite coupling.[24–26] We develop below a simpler approach that looks like an effective medium approximation (EMA), which will successfully estimate the shift of the optical absorption line as a function of the degree of disorder, and use the concept of motional narrowing[27] to estimate the line width.

A. Shift of the absorption spectra

The EMA approach simply consists of making the average over the realizations of disorder directly in Eq. (6) and replacing $\langle \Sigma_{\mathbf{m}} |\mathbf{r_n}-\mathbf{r_m}|^{-3} G_{\mathbf{m}}(t)\rangle$ by $\langle \Sigma_{\mathbf{m}} |\mathbf{r_n}-\mathbf{r_m}|^{-3}\rangle \times \langle G_{\mathbf{m}}(t)\rangle$. It might be correct for relatively small fluctuations of molecular positions ($\sigma \ll 1$), namely when small values of $|\mathbf{r_n}-\mathbf{r_m}|$ are not very probable. In doing so, we obtain the following equation of motion for the averaged Green function:

$$i\frac{d}{dt}\langle G(t)\rangle = J\mathcal{F}_{\text{eff}}\langle G(t)\rangle, \tag{16}$$

where the subscript has been dropped as the average of $G_{\mathbf{n}}(t)$ becomes independent of position. For brevity, we have defined

$$\mathcal{F}_{\text{eff}} \equiv \sum_{\mathbf{m}} \left\langle \frac{1}{|\mathbf{r_m}-\mathbf{r_0}|^3} \right\rangle. \tag{17}$$

Notice that both $\mathbf{r_m}$ and $\mathbf{r_0}$ fluctuate around regular positions. To determine $\mathcal{F}_{\text{eff}}$ we assume that $\mathbf{r_m}$ does not fluctuate but $\mathbf{r_0}$ fluctuates around the origin with deviation $\sqrt{2}\sigma$ along each direction. In addition, under the assumption of small degree of disorder ($|\mathbf{r_0}| \ll 1$), one can expand $|\mathbf{r_m}-\mathbf{r_0}|^{-3}$ in Taylor series. We then obtain

$$\mathcal{F}_{\text{eff}} = \mathcal{F}_3 + 9\mathcal{F}_5\sigma^2 + \tfrac{225}{2}\mathcal{F}_7\sigma^4 + \mathcal{O}(\sigma^6). \tag{18}$$

Using the value of $\mathcal{F}_l$ given in (12), the shift of the optical line is found to be

$$E(\sigma) - E(\sigma=0) = J(45.81\,\sigma^2 + 497.60\,\sigma^4), \tag{19}$$

for an infinite 2D lattice with dipole–dipole interaction. Note that the obtained scaling does not depend on the dimensionality since it yields the same quadratic σ-dependence of the absorption line shift reported in Ref. 14 for 1D configurationally disordered exciton systems and differs from the almost linear behavior found for 2D exciton systems with diagonal disorder.[28]

B. Broadening of the absorption spectra

In order to get insight into the broadening of the absorption spectra due to disorder, one should calculate the mean-square deviation of the exciton eigenenergies as well as the matrix of the exciton mode coupling. For the sake of simplicity, let us consider a square lattice and assume periodic boundary conditions so that, in the absence of disorder, Bloch plane waves represent the proper eigenfunctions of the Hamiltonian (1). Now, we rewrite the Hamiltonian (1) in the Bloch wave representation

$$\mathcal{H} = \sum_{\mathbf{k}} E_{\mathbf{k}} a_{\mathbf{k}}^{\dagger} a_{\mathbf{k}} + \sum_{\mathbf{k}\mathbf{k}'} (\delta\mathcal{H})_{\mathbf{k}\mathbf{k}'} a_{\mathbf{k}}^{\dagger} a_{\mathbf{k}'}, \tag{20}$$

where $\mathbf{k}$ ranges over the first Brillouin zone, $E_{\mathbf{k}}$ is given by Eq. (10), and

$$(\delta\mathcal{H})_{\mathbf{k}\mathbf{k}'} = \frac{J}{\mathcal{N}} \sum_{\mathbf{mn}} \left(\frac{1}{|\mathbf{m}-\mathbf{n}+\boldsymbol{\xi}_{\mathbf{m}}-\boldsymbol{\xi}_{\mathbf{n}}|^3} - \frac{1}{|\mathbf{m}-\mathbf{n}|^3} \right) \times e^{i(\mathbf{k}\cdot\mathbf{m}-\mathbf{k}'\cdot\mathbf{n})}. \tag{21}$$

The subject of our interest is precisely the matrix $(\delta\mathcal{H})_{\mathbf{k}\mathbf{k}'}$ and our task is to evaluate the following magnitude:

$$\sigma_{\mathbf{k}\mathbf{k}'}^2 = \langle (\delta\mathcal{H})_{\mathbf{k}\mathbf{k}'}^2 \rangle - \langle (\delta\mathcal{H})_{\mathbf{k}\mathbf{k}'} \rangle^2. \tag{22}$$

The diagonal part, $\sigma_{\mathbf{k}\mathbf{k}}$, determines the value of the typical fluctuation of the eigenenergy $E_{\mathbf{k}}$ due to disorder. For perturbative magnitudes of disorder, it has a direct relationship with the inhomogeneous width of the corresponding exciton state. The perturbative approach is valid provided the off-diagonal terms $\sigma_{\mathbf{k}\mathbf{k}'}$, describing the exciton level mixing, are smaller than the corresponding energy differences $|E_{\mathbf{k}} - E_{\mathbf{k}'}|$. From the viewpoint of the exciton optical response, coupling of the optically active exciton state $\mathbf{k}=\mathbf{0}=(0,0)$ to the others is of major importance. Therefore, the equality $\sigma_{\mathbf{k_1 0}} = E_{\mathbf{0}} - E_{\mathbf{k_1}}$, where the state $\mathbf{k_1}=(2\pi/N,0)$ is adjacent to the top state, separates the ranges of perturbative and nonperturbative magnitudes of the degree of disorder.

Assuming the smallness of the standard deviation σ and the long-wave limit $|\mathbf{k}| \ll 1$—the case of our interest—one can arrive at the following formula for $\sigma_{\mathbf{k}\mathbf{k}'}^2$ (see the Appendix for further details):

$$\sigma_{\mathbf{k}\mathbf{k}'}^2 = \frac{2520 J^2 \sigma^4}{\mathcal{N}}. \tag{23}$$

The $\mathcal{N}^{-1}$ scaling obtained is similar to that for 1D exciton system with diagonal disorder and is known as exchange or motional narrowing effect,[27] meaning $\mathcal{N}$-times reducing the variance of disorder distribution for a collective (excitonic) state as compared to the seeding value σ^2. What is most important, the σ-dependence, same as for 1D systems,[29] is sufficiently different: here, $\sigma_{\mathbf{k}\mathbf{k}'}^2$ is proportional to σ^4, while for diagonal disorder the corresponding magnitude scales as σ^2.[27] The latter behavior also appears when one simulates off-diagonal disorder by uncorrelated distributions of the nearest-neighbor hopping integrals.[16,30] The reason for the difference found lies in the fact that, despite assuming $\boldsymbol{\xi}_{\mathbf{n}}$ to be an uncorrelated stochastic variable for different sites $\mathbf{n}$, hopping integrals appear to be correlated. Indeed, let us consider for the sake of simplicity these integrals for the nearest neighbors, $J_{\mathbf{n}+\mathbf{g},\mathbf{n}}$ and $J_{\mathbf{n}-\mathbf{g},\mathbf{n}}$ ($|\mathbf{g}|=1$), and look at their fluctuations created by the deviation of $\mathbf{n}$th site up to linear terms in $\boldsymbol{\xi}_{\mathbf{n}}$. Evidently, $\delta J_{\mathbf{n}+\mathbf{g},\mathbf{n}} = 3\mathbf{g}\cdot\boldsymbol{\xi}_{\mathbf{n}}$, while $\delta J_{\mathbf{n}-\mathbf{g},\mathbf{n}} = -3\mathbf{g}\cdot\boldsymbol{\xi}_{\mathbf{n}}$, just confirming our claim. Due to this feature, they almost (or exactly at $\mathbf{k}=\mathbf{k}'$, see the Appendix) cancel each other in $(\delta\mathcal{H})_{\mathbf{k}\mathbf{k}'}$ when summing over neighboring sites in the long wavelength limit $|\mathbf{k}|, |\mathbf{k}'| \ll 1$. This is why the major contribution to $(\delta\mathcal{H})_{\mathbf{k}\mathbf{k}'}$ appears to be quadratic in σ.

For nonperturbative magnitudes of the disorder, $\sigma_{\mathbf{k}\mathbf{k}'}$ ($\mathbf{k} \neq \mathbf{k}'$) mixes the exciton states. This yields exciton localization within 2D regions of typical size $\mathcal{N}^* = N^* \times N^*$ smaller than $\mathcal{N} = N \times N$ and subsequently affects the exciton optical response. For a perfect lattice, only the state with $\mathbf{k}=\mathbf{0}$ is coupled to the light and carries the entire exciton oscillator strength, which is then $\mathcal{N} = N \times N$ times larger than that for an isolated molecule. Being mixed with other (nonradiative) states ($\mathbf{k} \neq \mathbf{0}$), the radiative state loses a part of the oscillator strength due to its spreading over the nonradiative ones. Thus, an effective number $\mathcal{N}^* < \mathcal{N}$, known as the num-

ber of coherently bound molecules for 1D excitons,[27] replaces the system size $\mathcal{N}$ as the enhancement factor of the oscillator strength of the localized exciton states. It reflects the typical number of sites on which the localized exciton wave functions have a significant magnitude or, in other words, the number of molecules within a typical localization area.[31,32] Accordingly, the inhomogeneous width of the optical exciton line will also be subject to renormalization and can now be estimated from $\sigma_{\mathbf{kk}}$ replacing $\mathcal{N}$ with $\mathcal{N}^*$.[27]

In our estimate of $\mathcal{N}^*$ we will follow a simple rule, first proposed in Ref. 33, that works fairly well for 1D exciton systems. This rule simply consists of applying the relation $\sigma_{\mathbf{k}_1\mathbf{0}}=E_{\mathbf{0}}-E_{\mathbf{k}_1}$, providing the limit of validity of the perturbative approach, to a typical localization area $N^*\times N^*$, i.e., replacing in this equality $\mathcal{N}$ with $\mathcal{N}^*$. It will give us the self-consistent equation for the size of the coherent area. First, let us look for $\mathcal{N}^*$ in the NN approximation. Taking into account Eqs. (13) and (23) and following the above rules, we then find

$$\mathcal{N}^*=\frac{2\pi^4}{315\sigma^4}, \tag{24a}$$

and consequently

$$\sigma^*_{\mathrm{NN}}=\left(\frac{2520}{\mathcal{N}^*}\right)^{1/2}J\sigma^2=\frac{630}{\pi^2}J\sigma^4. \tag{24b}$$

Equations (24a) and (24b) provide estimates of the oscillator strength and the standard deviation of the absorption line at nonperturbative magnitudes of disorder. We stress that the scaling of $\sigma^*_{\mathrm{NN}}\propto\sigma^4$ dramatically differs from that found for 2D exciton systems with diagonal disorder, for which $\sigma^*_{\mathrm{NN}}\propto\sigma$.[28]

Turning now to the case of long-range interactions and making estimates as above, we arrive at a surprising result, namely, that the quantity $\mathcal{N}^*$ we are looking for falls out of the equation determining it. This occurs because both $E_{\mathbf{k}}$ and $\sigma_{\mathbf{kk}'}$ scale as $\mathcal{N}^{-1/2}$. Finally, we get an estimate $\sigma^*_{\mathrm{LR}}=2\pi/(2520)^{1/4}\simeq 0.89$ for the magnitude of the degree of disorder, which separates the perturbative and nonperturbative ranges of σ. Within the perturbative range ($\sigma\ll\sigma^*_{\mathrm{LR}}$), exciton eigenfunctions spread over the whole lattice so that $\mathcal{N}^*=\mathcal{N}$. The inhomogeneous width of exciton levels is still given by $\sigma_{\mathbf{kk}}$. At nonperturbative magnitudes of disorder ($\sigma\geqslant\sigma^*_{\mathrm{LR}}$), Eq. (23) fails since for its derivation, the condition $\sigma\ll 1$ has been used (see the Appendix). Therefore, $\sigma_{\mathbf{kk}'}$ should be recalculated for $\sigma\geqslant\sigma^*_{\mathrm{LR}}$ but it is not the case we will be dealing with.

C. Numerical simulation

For the magnitudes of the degree of disorder $\sigma\leqslant 0.08$ and lattice size $\mathcal{N}=20\times 20$ we used in our simulations of the absorption spectra of disordered lattices, the corresponding motionally reduced values are $\sigma_{\mathbf{kk}'}<0.016$. Thus, despite the seeding, disorder is rather strong (the standard deviation of the nearest-neighbor hopping integral for the 2D case is given by $\sigma_J=6\sigma J$ and for $\sigma=0.08$ is equal to 0.48), the quantity $\sigma_{\mathbf{kk}'}$ drops to perturbative values (unlike the 1D case[14]). This requires tiny values of the dissipation parameter α in Eq. (4) to observe line broadening which, in turn, drastically increases the computation time. Hence, we have directly diagonalized the Hamiltonian (1) to find the exciton absorption spectra. We then use Eq. (3) to find the absorption line shape, where we replaced $\delta(E-E_k)$ by $(1/R)\theta(R/2-|E-E_k|)$, θ being the Heaviside step function and R the spectral resolution.[14] Different values of the degree of disorder σ have been studied and each spectrum shown in the figures below corresponds to an average over 2000 realizations of disorder. In all the simulations, we have chosen $J=1$ and $R=0.001$.

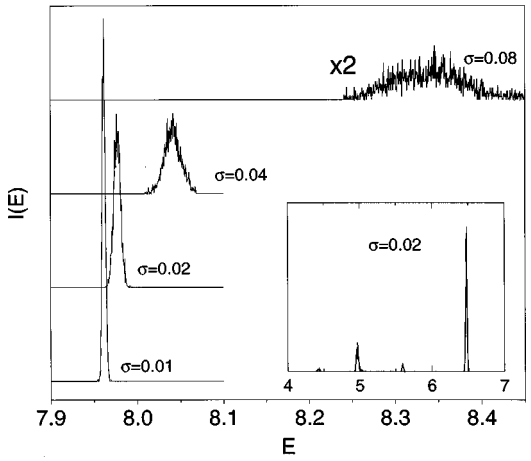

FIG. 2. Absorption spectra in arbitrary units for 20×20 disordered lattices when dipole–dipole interaction between all sites is taken into account. Curves are calculated by diagonalization of the Hamiltonian with $J=1$ and $R=0.001$ and comprise the results of 2000 averages. The inset shows the low-energy satellite peaks for $\sigma=0.02$.

Figure 2 shows the absorption spectra of 20×20 disordered lattices when dipole–dipole interaction between all sites is taken into account for different values of the degree of disorder. Notice that the main line shifts towards the high-energy region of the spectrum on increasing the degree of disorder. In addition, the main line is rapidly broadened upon increasing the degree of disorder, in agreement with the analytical results shown in the previous section. Besides the main absorption line, several satellite peaks appear in the low-energy side of the spectra, resembling those found in ordered lattices. As an example, the inset of Fig. 2 presents the satellite peaks closest to the main absorption line for $\sigma=0.02$. As expected, these satellite peaks are also shifted to the high-energy region and broadened due to disorder. The invariance of relative positions of the main peak and satellites (they match those for an ordered lattice of the same size, see Fig. 1) is explained by the low magnitudes of $\sigma_{\mathbf{kk}'}<0.016$, being unable to mix the exciton states of perfect lattice. Notice once more that the conditions of our simulations correspond to the perturbative limit of disorder. Unfortunately, higher values of σ make the occurrence of small values of the nearest-neighbor distance highly probable, thus leading to huge hopping integrals and blowup of numerics.

For comparison, Fig. 3 presents the behavior of the absorption spectra for 20×20 lattices upon increasing the degree of disorder σ within the NN approximation. The main line again is blueshifted and broadened upon increasing the

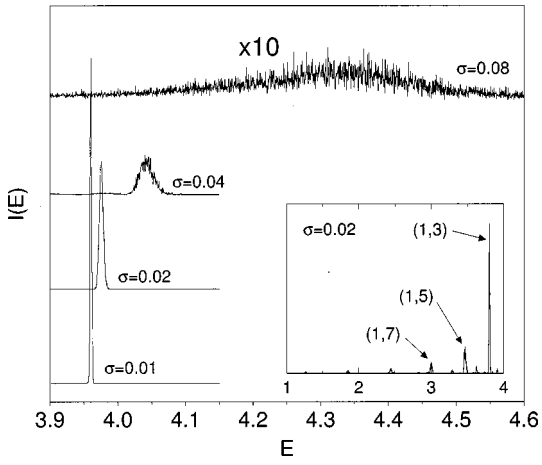

FIG. 3. Absorption spectra in arbitrary units for 20×20 disordered lattices within the NN approximation. Curves are calculated by diagonalization of the Hamiltonian with $J=1$ and $R=0.001$ and comprise the results of 2000 averages. The inset shows the low-energy satellite peaks for $\sigma=0.02$.

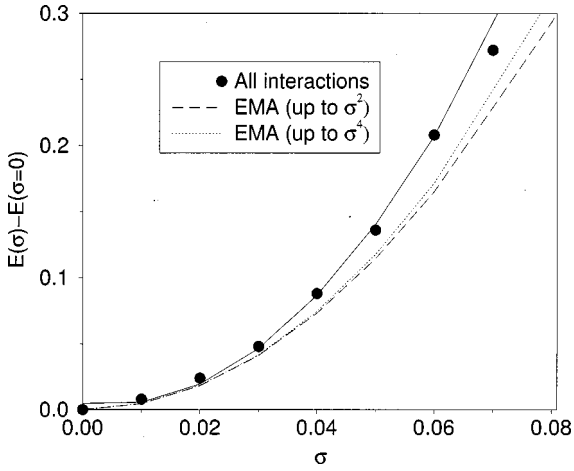

FIG. 4. Shift in energy of the main absorption line versus σ when dipole–dipole interaction between different sites is taken into account. Solid line is the result of quadratic fit. Dashed and dotted lines show EMA prediction up to orders σ^2 and σ^4, respectively.

degree of disorder. For $\sigma\leqslant 0.04$, its width (at a fixed σ) is almost the same as for the case when the full dipole–dipole interaction is taken into account, but it is larger for higher values of the degree of disorder. An extra broadening of the absorption line occurs, indicating that the disorder starts to mix the exciton states which results in their localization within an area of size smaller than the lattice size. Now, the number $\mathcal{N}^*<\mathcal{N}$ determines the inhomogeneous line width. This point will be discussed in more detail below. The main line is accompanied by satellite peaks, as the inset of Fig. 3 shows for $\sigma=0.02$. The locations of all of them perfectly follow Eq. (13), in which $\mathbf{k}$ should be taken of the form $\mathbf{k}=[\pi\nu_x/(N+1),\pi\nu_y/(N+1)]$ with $\nu_x,\nu_y=1,2,...,N$. For instance, for $\sigma=0.02$, the highest satellite peaks correspond to the set (1,3), (1,5), (1,7), ... Besides, there exists a number of satellite peaks with even ν_x or ν_y indices whose 1D counterpart has vanishing oscillator strength and, consequently, they present very low intensity [see, e.g., the satellite peak closest to $E=3.9$, whose indices are (1,2)]. Such peaks are not present in ordered lattices with the NN intersite coupling. Hence, we relate their appearance to mixing of the optically active states ($\nu_{x,y}=1$) with the dark ones (with $\nu_{x,y}$ even) caused by disorder.

Figure 4 compares the shift of the main line obtained numerically with the EMA prediction given in (19), where we observe a nonlinear shift upon increasing the degree of disorder. We see that the EMA works very well for $\sigma\leqslant 0.03$ but underestimates the value of the shift for strong disorder. This is to be expected since we assumed that σ was small to arrive at Eq. (19). Additional terms in the expansion (18) as a function of powers of σ^2 provide positive contributions leading to a larger shift.

Finally, we have also obtained the full width at half maximum (FWHM) of the main absorption line to analyze its dependence on the degree of disorder. The results for both models, when the dipole–dipole interaction between all sites is taken into account as well as within the NN approximation, are shown in Fig. 5(a), where the value of the spectral resolution has been subtracted. As was already mentioned, for a fixed σ smaller than 0.04, the FWHM is almost the same in both models but the curves clearly start to separate for higher values of the degree of disorder. We have found that for the model of full dipolar coupling, the FWHM can be accurately fitted over the entire range of the degree of disorder considered in this work by a power law $a\sigma^{\gamma}$ with $a=25$ and $\gamma=1.79$. The exponent 1.79 is rather close to the value of 2 expected from our theoretical estimates. On the contrary, the FWHM of the main absorption line obtained within the NN approximation does not fit a single power law, at it follows from Fig. 5(a). The exponent $\gamma=1.93$ found for small degree of disorder ($\sigma<0.04$) is close to 2, but it turns out to be roughly 3.78 for stronger disorder ($\sigma>0.04$). The value $\gamma=3.78$ is again in good agreement with our theoretical estimate (24b) for nonperturbative magnitudes of the degree of disorder.

We conjectured above that, within the NN approximation, disorder starts to mix the exciton states at $\sigma>0.04$ resulting in their localization. To validate this assertion we have also calculated the inverse participation ratio (IPR) of

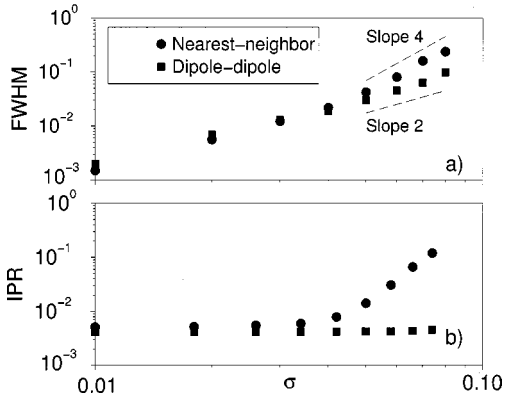

FIG. 5. (a) FWHM of the main absorption line and (b) IPR of the uppermost state versus σ. Curves are calculated by diagonalization of the Hamiltonian with $J=1$ and comprise the results of 2000 averages. The dashed lines represent the theoretical slopes 2 and 4.

the uppermost exciton state $\Psi_{\nu\mathbf{n}}$ according to the standard definition IPR$=\Sigma_{\mathbf{n}}|\Psi_{\nu\mathbf{n}}|^4$, where the wave function is assumed to be properly normalized (see, e.g., Ref. 34). For delocalized states, spreading uniformly over the 2D system, the IPR behaves like N^{-2} upon increasing the lateral size N. On the contrary, localized states exhibit much higher values: the higher the value, the smaller the localization length. The results are shown in Fig. 5(b). For the model of dipolar coupling between all sites, the IPR is approximately constant over the entire range of σ. Its value is close to the theoretical expectation 0.0025 for delocalized states in 20×20 systems. Within the NN approximation, the IPR suddenly increases for $\sigma>0.04$, meaning that the exciton starts to be localized, in perfect agreement with our previous conjecture.

VI. SUMMARY

Coupling to far neighbors has pronounced effects on the one-exciton absorption spectra of perfect 2D lattices. In the case of positive sign of the dipole–dipole coupling considered in the present paper, the absorption spectrum consists of the main peak and almost equidistantly placed redshifted satellites of decreasing intensities. These satellites reflects a linear dispersion law of the exact 2D exciton energy spectrum unlike the parabolic law of the NN problem. The main peak is blueshifted approximately twice as compared to that arising in the NN approximation. Introducing Gaussian configurational disorder yields a blueshift of the main peak of the exciton absorption spectrum, obeying a polynomial biquadratic law with respect to the degree of configurational disorder as well as broadening all the peaks.

The motional narrowing effect in the case of Gaussian configurational disorder sufficiently differs from that of diagonal disorder. Being similar to the latter in the scaling law with respect to the number of sites ($\sim\mathcal{N}^{-1/2}$), the former is different in the dependence on the degree of disorder σ, giving rise to a parabolic behavior, contrary to the linear one found for diagonal disorder. As a result, motionally reduced disorder appears to have perturbative magnitudes, even for relatively large values of the standard deviation of molecular positions.

ACKNOWLEDGMENTS

The authors thank R. Brito for helpful comments. Work at Madrid was supported by CAM under Project No. 07N/0034/98. V.A.M. thanks UCM for the support under Sabáticos Complutense.

APPENDIX: ESTIMATE OF THE MOTIONAL NARROWING EFFECT IN THE PRESENCE OF CONFIGURATIONAL DISORDER

In what follows, we assume the smallness of the standard deviation σ and expand the quantity in parentheses in Eq. (21) in the Taylor series up to fourth order with respect to

$$X_{\mathbf{mn}}=\frac{2(\mathbf{m}-\mathbf{n})\cdot(\boldsymbol{\xi}_{\mathbf{m}}-\boldsymbol{\xi}_{\mathbf{n}})}{|\mathbf{m}-\mathbf{n}|^2}+\frac{|\boldsymbol{\xi}_{\mathbf{m}}-\boldsymbol{\xi}_{\mathbf{n}}|^2}{|\mathbf{m}-\mathbf{n}|^2}.$$

We will be interested in the contribution to $\sigma^2_{\mathbf{kk}'}$ up to the same order with respect to σ. The corresponding expressions read

$$(\delta\mathcal{H})_{\mathbf{kk}'}=\frac{J}{\mathcal{N}}\sum_{\mathbf{mn}}\frac{e^{i(\mathbf{k}\cdot\mathbf{m}-\mathbf{k}'\cdot\mathbf{n})}}{|\mathbf{m}-\mathbf{n}|^3}\times\left(-\frac{3}{2}X_{\mathbf{mn}}+\frac{15}{8}X^2_{\mathbf{mn}}-\frac{35}{16}X^3_{\mathbf{mn}}+\frac{315}{128}X^4_{\mathbf{mn}}\right),\tag{A1a}$$

and consequently

$$(\delta\mathcal{H})^2_{\mathbf{kk}'}=\left(\frac{J}{\mathcal{N}}\right)^2\sum_{\mathbf{mn}}\frac{e^{i(\mathbf{k}\cdot\mathbf{m}-\mathbf{k}'\cdot\mathbf{n})}}{|\mathbf{m}-\mathbf{n}|^3}\sum_{\mathbf{pq}}\frac{e^{-i(\mathbf{k}\cdot\mathbf{p}-\mathbf{k}'\cdot\mathbf{q})}}{|\mathbf{p}-\mathbf{q}|^3}\times\left(\frac{9}{4}X_{\mathbf{mn}}X_{\mathbf{pq}}-\frac{45}{8}X_{\mathbf{mn}}X^2_{\mathbf{pq}}+\frac{105}{16}X_{\mathbf{mn}}X^3_{\mathbf{pq}}+\frac{225}{64}X^2_{\mathbf{mn}}X^2_{\mathbf{pq}}\right).\tag{A1b}$$

Carrying out the average in Eq. (A1) and keeping all the necessary terms, we obtain (the calculations are rather tedious but straightforward, so that we only quote the final result)

$$\langle(\delta\mathcal{H})_{\mathbf{kk}'}\rangle=[9JQ_5(\mathbf{k})\sigma^2+\tfrac{225}{2}Q_7(\mathbf{k})\sigma^4]\delta_{\mathbf{kk}'},\tag{A2a}$$

$$\langle(\delta\mathcal{H})^2_{\mathbf{kk}'}\rangle=\frac{9J^2\sigma^2}{\mathcal{N}}|\mathbf{P}_5(\mathbf{k})+\mathbf{P}^*_5(\mathbf{k}')|^2-\frac{36J^2\sigma^4}{\mathcal{N}}\times[Q_5(\mathbf{k})+Q_5(\mathbf{k}')]^2+\frac{153J^2\sigma^4}{\mathcal{N}}\times[Q_{10}(0)+Q_{10}(\mathbf{k}+\mathbf{k}')]^2+\frac{225J^2\sigma^4}{2\mathcal{N}}R(\mathbf{k},\mathbf{k}')+\frac{270J^2\sigma^4}{\mathcal{N}}\times[\mathbf{P}_5(\mathbf{k})+\mathbf{P}^*_5(\mathbf{k}')][\mathbf{P}^*_7(\mathbf{k})+\mathbf{P}_7(\mathbf{k}')]+81\sigma^4Q^2_5(\mathbf{k})\delta_{\mathbf{kk}'},\tag{A2b}$$

where the functions $Q_l(\mathbf{k})$, $P_l(\mathbf{k})$, and $R(\mathbf{k},\mathbf{k}')$ are given by

$$Q_l(\mathbf{k})=\sum_{\mathbf{m}}\frac{e^{i\mathbf{k}\cdot\mathbf{m}}}{|\mathbf{m}|^l},\tag{A3a}$$

$$\mathbf{P}_l(\mathbf{k})=\sum_{\mathbf{m}}\frac{\mathbf{m}e^{i\mathbf{k}\cdot\mathbf{m}}}{|\mathbf{m}|^l},\tag{A3b}$$

$$R(\mathbf{k},\mathbf{k}')=\sum_{\mathbf{mn}}\frac{(\mathbf{m}\cdot\mathbf{n})^2}{|\mathbf{m}|^7|\mathbf{n}|^7}(e^{i\mathbf{k}\cdot\mathbf{m}}+e^{i\mathbf{k}'\cdot\mathbf{m}})(e^{i\mathbf{k}\cdot\mathbf{n}}+e^{i\mathbf{k}'\cdot\mathbf{n}}).\tag{A3c}$$

For the magnitude of interest, we get

$$\sigma^2_{\mathbf{k}\mathbf{k}'} = \frac{9J^2\sigma^2}{\mathcal{N}}\left|\mathbf{P}_5(\mathbf{k}) + \mathbf{P}_5^*(\mathbf{k}')\right|^2 - \frac{36J^2\sigma^4}{\mathcal{N}} \times [Q_5(\mathbf{k}) + Q_5(\mathbf{k}')]^2 + \frac{153J^2\sigma^4}{\mathcal{N}} \times [Q_{10}(0) + Q_{10}(\mathbf{k}+\mathbf{k}')]^2 + \frac{225J^2\sigma^4}{2\mathcal{N}} R(\mathbf{k},\mathbf{k}') + \frac{270J^2\sigma^4}{\mathcal{N}}[\mathbf{P}_5(\mathbf{k}) + \mathbf{P}_5^*(\mathbf{k}')][\mathbf{P}_7^*(\mathbf{k}) + \mathbf{P}_7(\mathbf{k}')]. \tag{A4}$$

From the viewpoint of our problem, the domain of importance of the wave numbers $\mathbf{k}$ and $\mathbf{k}'$ is represented by their smaller magnitudes. In this regard, it should be stressed that, despite the lowest term of $\sigma^2_{\mathbf{k}\mathbf{k}'}$ with respect to the seeding degree of disorder is of order σ^2, the main contribution to $\sigma^2_{\mathbf{k}\mathbf{k}'}$ is determined by the terms of fourth order in σ. Indeed, for $\mathbf{k}=\mathbf{k}'$ this statement is rigorous since $\mathbf{P}_l(\mathbf{k}) + \mathbf{P}_l^*(\mathbf{k}) \equiv 0$. On the other hand, as follows from the definitions (A3), $\mathbf{P}_l(\mathbf{k}=\mathbf{0}) = 0$, which means that the corresponding terms in Eq. (A4) have an additional suppression factor proportional to $\mathbf{k}^2 \sim \mathcal{N}^{-1}$. Therefore, they can be neglected as compared to other terms, keeping in mind that $\mathcal{N}$ is large enough. Estimating the rest of the functions in Eq. (A4) as follows, $Q_l(\mathbf{k}\to\mathbf{0}) \approx 4$ and $R(\mathbf{k},\mathbf{k}'\to\mathbf{0}) \approx 32$, we arrive finally at Eq. (23).

[1] A. S. Davydov, *Theory of Molecular Excitons* (Plenum, New York, 1971).
[2] F. C. Spano and J. Knoester, in *Advances in Magnetic and Optical Resonance*, edited by W. S. Warren (Academic, New York, 1994), Vol. 18, p. 117.
[3] *J-Aggregates*, edited by T. Kobayashi (World Scientific, Singapore, 1996), p. 111.
[4] J. Terpstra, H. Fidder, and D. A. Wiersma, Chem. Phys. Lett. **179**, 349 (1991).
[5] H. Fidder, Ph.D. thesis, Groningen, 1993.
[6] A. Nabetani, A. Tamioka, H. Tamuru, and K. Miyano, J. Chem. Phys. **102**, 5109 (1995).
[7] D. Möbius, Adv. Mater. **7**, 437 (1995).
[8] S. Engelhard and F. H. M. Faisal, J. Chem. Phys. **110**, 3596 (1999).
[9] K. Zhu and T. Kobayashi, Phys. Lett. A **196**, 105 (1994).
[10] Y. Xiao and W.-H. Hai, Phys. Lett. A **209**, 99 (1995).
[11] V. V. Konotop and S. Takeno, Phys. Rev. B **55**, 11 342 (1997).
[12] V. V. Konotop, M. Salerno, and S. Takeno, Phys. Rev. E **56**, 7240 (1997).
[13] P. L. Christiansen, Yu. B. Gaididei, M. Johansson, K. Ø. Rasmussen, V. K. Mezentsev, and J. Juul Rasmussen, Phys. Rev. B **57**, 11 303 (1998).
[14] H. Fidder, J. Knoester, and D. A. Wiersma, J. Chem. Phys. **95**, 7880 (1991).
[15] V. Malyshev and P. Moreno, Phys. Rev. B **51**, 14587 (1995).
[16] G. G. Kozlov, V. A. Malyshev, F. Domínguez-Adame, and A. Rodríguez, Phys. Rev. B **58**, 5367 (1998).
[17] V. A. Malyshev, A. Rodríguez, and F. Domínguez-Adame, J. Lumin. **81**, 127 (1999).
[18] J.-P. Lemaistre, J. Lumin. **76–77**, 437 (1998).
[19] D. L. Huber and W. Y. Ching, Phys. Rev. B **39**, 8652 (1989).
[20] M. L. Glasser, J. Math. Phys. **14**, 409 (1973).
[21] R. J. Elliott, J. A. Krumhansl, and P. L. Leath, Rev. Mod. Phys. **46**, 465 (1974).
[22] D. L. Huber, Chem. Phys. **128**, 1 (1988).
[23] A. Boukahil and D. L. Huber, J. Lumin. **45**, 13 (1990).
[24] R. A. Tahir-Kheli, Phys. Rev. B **6**, 2808 (1972); **6**, 2826 (1972); **6**, 2838 (1972).
[25] I. Avgin, D. L. Huber, and W. Y. Ching, Phys. Rev. B **46**, 223 (1992); **48**, 16109 (1993).
[26] I. Avgin and D. L. Huber, Phys. Rev. B **48**, 13625 (1993).
[27] E. W. Knapp, Chem. Phys. **85**, 73 (1984).
[28] M. Schreiber and Y. Toyozawa, J. Phys. Soc. Jpn. **51**, 1528 (1982).
[29] V. A. Malyshev and F. Domínguez-Adame, Chem. Phys. Lett. **313**, 255 (1999).
[30] A. Tilgner, H. P. Tromsdorf, J. M. Zeigler, and R. M. Hochstrasser, J. Lumin. **45**, 373 (1990); J. Chem. Phys. **96**, 781 (1992).
[31] J. M. Rorison and D. C. Herbert, Superlattices Microstruct. **1**, 423 (1985).
[32] J. Feldmann, G. Peter, E. O. Göbel, P. Dawson, K. Moore, C. Foxon, and R. J. Elliott, Phys. Rev. Lett. **59**, 2337 (1987).
[33] V. A. Malyshev, Opt. Spektrosk. **71**, 873 (1991); [Opt. Spectrosc. **71**, 505 (1991)]; J. Lumin. **55**, 225 (1993).
[34] J. Canisius and J. L. van Hemmen, J. Phys. C **18**, 4873 (1985).